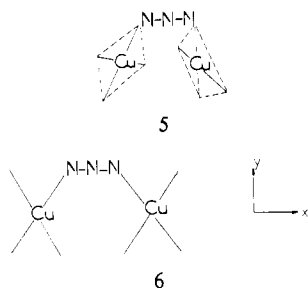
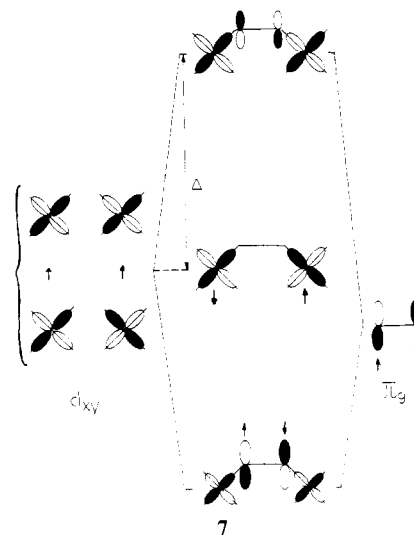


localized¹⁵ make a dihedral angle of 46° as schematized in 5; in the other complexes, these basal planes are coplanar as shown in 6.



The key role in the strong stabilization of the singlet state observed with end-to-end azido bridges is played by the π_g HOMO's of N_3^- (see 7).^{4,6} The interaction between these π_g 's and the d_{xy} metal orbitals give rise to the following: (i) An antibonding MO, antisymmetric regarding the mirror plane perpendicular to the azido bridge, appears. This MO is destabilized by an energy, Δ , with regard to the xy -type MO, symmetric regarding the mirror plane. The larger Δ is, the more stabilized the singlet state. More precisely, in absence of any other effect, the magnitude of the antiferromagnetic interaction varies as Δ^2 . This is an *active electron effect*. (ii) A bonding MO appears in which an electron of π_g with an α spin is delocalized toward one of the copper(II) ions (e.g. A) and the other electron with the β spin is delocalized toward the other copper(II) ion (B). Hence, the unpaired electron around A will have a probability of spin β larger than $1/2$ and the unpaired electron around B a probability of a spin α larger than $1/2$, which favors the singlet state as ground state. This



is the so-called *spin polarization effect*. Both, the active electron effect and the spin polarization effect favor the singlet state as ground state. As usual in copper(II) binuclear complexes, the phenomenon is enhanced when the two xy -type metal orbitals are localized in the same plane.¹⁵ That is why the in-plane situation 6 is more favorable than the out-of-plane situation 5.

Registry No. $[Cu_2(tmen)_2(N_3)_3](PF_6)$, 93255-78-8.

Supplementary Material Available: Listings of structure factor amplitudes, bond distances and angles (Tables VI and VII), and anisotropic thermal parameters (Table VIII) (26 pages). Ordering information is given on any current masthead page.

Contribution from the Department of Chemistry, Seton Hall University, South Orange, New Jersey 07079, and Laboratoire de Chimie Analytique et Radiochimie (B6), University of Liege, Sart Tilman, B-4000 Liege, Belgium

Luminescence and NMR Studies of the Conformational Isomers of Lanthanide Complexes with an Optically Active Polyaza Polycarboxylic Macrocycle

HARRY G. BRITAIN*† and JEAN F. DESREUX**†

Received February 21, 1984

A variety of luminescence techniques were used to study the nature of the complexes formed between [1*R*-(1*R**,4*R**,7*R**,10*R**)]- $\alpha,\alpha',\alpha'',\alpha'''$ -tetramethyl-1,4,7,10-tetraazacyclododecane-1,4,7,10-tetraacetic acid (abbreviated as DOTMA) and several lanthanide ions. High-resolution luminescence spectra of EuDOTMA as a microcrystalline powder and in the aqueous phase clearly demonstrated that while a single Eu(III) species exists in the solid state, two nonequivalent species exist in solution. The circularly polarized luminescence spectrum of EuDOTMA showed only small degrees of observable optical activity in the species thought to be axially symmetric and large amounts of chirality in the species not possessing such symmetry. Comparison of the ground- and excited-state optical activities of TbDOTMA revealed that essentially no geometrical changes accompany the promotion of the Tb(III) ion into an excited f state. The exchange between the two complex isomers was found to be slow on the NMR time scale, and thus it was possible to deduce the structures of the two isomers. The relative concentrations of all the solution species were found to depend on the size of the lanthanide ion and on the functional groups present on the macrocycle. Finally, the DOTMA compounds were shown to be very rigid, with the conformation of the ethylenediamine groups of the macrocyclic ring undergoing a very slow inversion between 0 and 100 °C.

Introduction

The complexing abilities of macrocyclic ligands have led to numerous investigations in the coordination properties of these molecules. Generally, a wide variety of cations are capable

of being bound by a macrocycle, but most of these studies have been restricted to the alkali-metal and alkaline-earth ions. Since the report by King and Heckley¹ that lanthanide compounds of macrocyclic polyethers could be formed, the efforts of many investigators have led to the synthesis of new compounds with intriguing properties. These investigations have

*Seton Hall University.
†University of Liege.

(1) King, R. B.; Heckley, P. R. *J. Am. Chem. Soc.* 1974, 96, 3118.

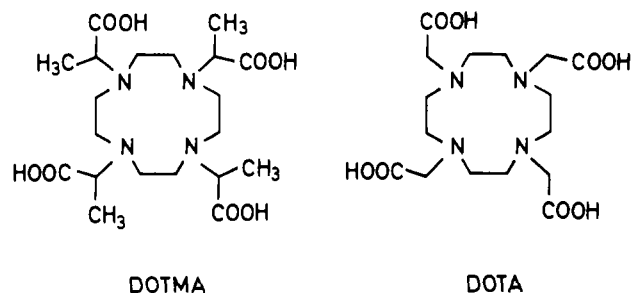


Figure 1. Structures of the DOTA and DOTMA ligands.

been spurred by the facts that several lanthanide macrocyclic complexes might function as effective NMR shift reagents for aqueous systems and that these compounds possess solution-phase structures that are readily predictable.

One particularly interesting macrocycle is 1,4,7,10-tetraazacyclododecane-1,4,7,10-tetraacetic acid (abbreviated as DOTA and whose structure is shown in Figure 1), since this ligand is known to form exceedingly stable complexes with calcium^{2,3} and lanthanide ions.⁴ The lanthanide compounds are even more unusual in that they are known to be axially symmetric and rigid on the NMR time scale, two rare features in lanthanide solution chemistry.⁴ The lanthanide DOTA compounds have been shown to function as effective NMR shift reagents,⁵ and luminescence studies have indicated that this activity may be traced to the presence of a labile water molecule present in the inner coordination sphere.^{6,7} The presence of a bound water molecule has been confirmed from the crystal structure of Na(EuDOTA·H₂O)·4H₂O, in which it was determined that the coordination polyhedron of the Eu(III) ion could best be described as that of a distorted monocapped square antiprism.⁸

The utility of chiroptical methods as a means for the study of optically active lanthanide compounds has become well established,⁹ and it is clearly desirable to examine the chirality of lanthanide compounds possessing well-defined geometries. To achieve such an end, a macrocycle closely resembling DOTA has been prepared that contains four asymmetric atoms. The structure of [1*R*-(1*R**,4*R**,7*R**,10*R**)]- $\alpha,\alpha',\alpha'',\alpha'''$ -tetramethyl-1,4,7,10-tetraazacyclododecane-1,4,7,10-tetraacetic acid (abbreviated as DOTMA) is also shown in Figure 1. One would anticipate that DOTMA would bind a lanthanide ion in a manner identical with that already known for the DOTA complexes. The chirality associated with the TbDOTMA and EuDOTMA complexes has been studied by means of circularly polarized luminescence (CPL) spectroscopy, and a variety of other photophysical techniques have been used to obtain additional information regarding these complexes.

Furthermore, the solution structure of the paramagnetic YbDOTMA compound has been established by NMR methods. These studies afforded an opportunity to probe questions already raised in previous investigations:^{5,6} Are the lanthanide polyaza polyacetate complexes involved in a slow equilibrium between conformational isomers? If so, what are the structures of these isomers? It has not been possible thus far to answer these questions in the case of complexes containing noncyclic

ligands due to the high lability and low symmetry of the compounds.

Experimental Section

The DOTMA ligand was prepared by a slightly modified approach to the condensation method already reported for DOTA,⁴ involving a Walden inversion that is essentially quantitative. The preparation of the starting materials followed previously outlined procedures. (*S*)-2-chloropropanoic acid was obtained by the method of Fu et al.,¹⁰ and 1,4,7,10-tetraazacyclododecane tetrahydrochloride was synthesized according to the method of Atkins and co-workers.¹¹ In a typical synthesis, 10.74 g (9.9 mmol) of (*S*)-2-chloropropanoic acid was dissolved in 10 mL of water and neutralized by a 10 M NaOH solution (the temperature was kept below 5 °C). At the same time, an aqueous solution containing 7.0 g (2.2 mmol) of the tetraaza macrocyclic salt was neutralized by the addition of 3.5 g (8.8 mmol) of NaOH dissolved in 5 mL of water. The two solutions were mixed, and the temperature was brought to 80 °C. A solution containing 4 g (10 mmol) of NaOH in 3.5 mL of water was then added dropwise to the stirred mixture over a period of 12 h. The pH should not exceed 10 at the beginning of the addition. After cooling, the pH was lowered to 2 with 12 M HCl, and the mixture was taken to dryness under vacuum. The remaining yellowish solid was suspended in 300 mL of ethanol, and after 3 h of agitation, the suspension was filtered and the solvent removed from the filtrate (rotary evaporator). The solid obtained in this manner was recrystallized three times in a 1:1 ethanol-water mixture. Yield: 2.23 g (22%). The purity of the ligand was checked by pH titrations. For the tetraprotonated form of DOTMA in water, it was determined that $[\alpha]^{20^\circ\text{C}}_{\text{D}} = -87.6^\circ$ at $c = 0.0776$ g/mL.

The lanthanide DOTMA complexes were prepared as 0.01 or 0.1 M solutions through the addition of aliquots of stock solutions of lanthanide chlorides to stoichiometric amounts of solid DOTMA. The resulting mixtures were heated to 80 °C, and a dilute NaOH solution was added until the pH reached 6.5. Water was stripped off on a rotary evaporator, and the required amount of H₂O or D₂O was then added. Crystals were obtained by allowing ethanol to diffuse into a concentrated aqueous solution of the lanthanide complexes.

Possible formation of polynuclear complexes in the aqueous solutions was investigated through a study of the intermolecular energy transfer from a TbDOTMA donor complex to an EuDOTMA acceptor complex. In these experiments, microliter amounts of a EuDOTMA solution were added to 3.0 mL of the TbDOTMA solution, with the emission intensity associated with the ⁵D₄ → ⁷F₅ band system (at 545 nm) being measured after each addition. The TbDOTMA compound was excited with the 488-nm output of a 5-W Ar ion laser (corresponding to the ⁷F₆ → ⁵D₄ absorption of Tb), as the Eu(III) ion is known to exhibit absolutely no absorption at this wavelength. Thus any quenching of the Tb(III) species must be exclusively due to an energy-transfer process. The emission lifetime of the TbDOTMA complex was also measured after each addition of EuDOTMA. In this measurement, the complex was excited by the 337-nm output of a nitrogen laser, with the decay curve being captured on a storage oscilloscope. The digitized decay curve was analyzed through standard least-squares techniques. In no case was more than a single exponential ever observed in any of the decay curves.

All CPL and total luminescence (TL) measurements were obtained on apparatus constructed in our laboratory, whose operation has been described.¹² In most cases, an excitation wavelength of 350 nm (UV output of the 5-W Ar ion laser) was employed. Measurements of the TL and CPL spectra were carried out simultaneously within the ⁵D₀ → ⁷F_{*J*} (*J* = 0–4) band systems of EuDOTMA and within the ⁵D₄ → ⁷D_{*J*} (*J* = 6–0) band systems of TbDOTMA. The emission was analyzed by a 0.5-m grating monochromator at 5-Å resolution, and it was determined that further increases in resolving power did not yield a significant improvement in the spectral features.

Excitation spectra of the TbDOTMA and EuDOTMA complexes were obtained on a Spex Fluorolog instrument, operating in the 2:2:2 configuration. The number of water molecules bound in the inner coordination sphere of the DOTMA complexes was determined from studies of the emission lifetimes of the compounds dissolved in H₂O and D₂O, following the procedures detailed by Horrocks et al.¹³

(2) Stetter, C. C.; Franck, W.; Mertens, R. *Tetrahedron* **1981**, *37*, 767.

(3) Delgado, R.; Fausto da Silva, J. J. R. *Talanta* **1982**, *29*, 815.

(4) Desreux, J. F. *Inorg. Chem.* **1980**, *19*, 1319.

(5) Bryden, C. C.; Reilley, C. N.; Desreux, J. F. *Anal. Chem.* **1981**, *53*, 1418.

(6) Albin, M.; Horrocks, W. D.; Liotta, F. J. *Chem. Phys. Lett.* **1982**, *85*, 61.

(7) Bryden, C. C.; Reilley, C. N. *Anal. Chem.* **1982**, *54*, 610.

(8) Spirlet, M.-R.; Rebizant, J.; Desreux, J. F.; Loncin, M.-F. *Inorg. Chem.* **1984**, *23*, 359.

(9) Brittain, H. G. *Coord. Chem. Rev.* **1983**, *48*, 243.

(10) Fu, S.-C. J.; Birnbaum, S. M.; Greenstein, J. P. *J. Am. Chem. Soc.* **1954**, *76*, 6054.

(11) Atkins, T. J.; Richman, J. E.; Oettle, W. F. *Org. Synth.* **1978**, *58*, 86.

(12) Brittain, H. G. *J. Am. Chem. Soc.* **1980**, *102*, 3693.

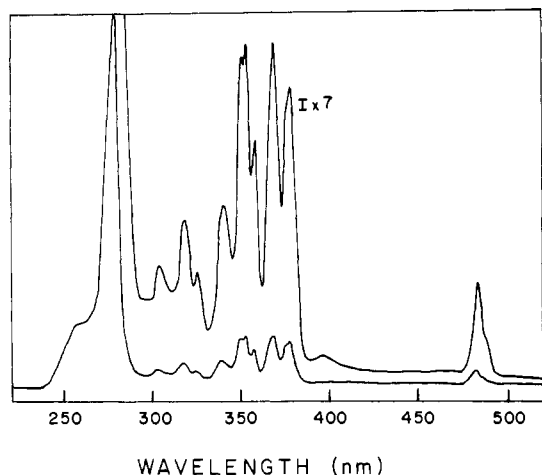


Figure 2. Excitation spectra of TbDOTMA, obtained at an emission wavelength of 544 nm. The intense feature at 281 nm is a Tb(III) f-d transition. The region containing the f-f excitation peaks has been expanded by a factor of 7.

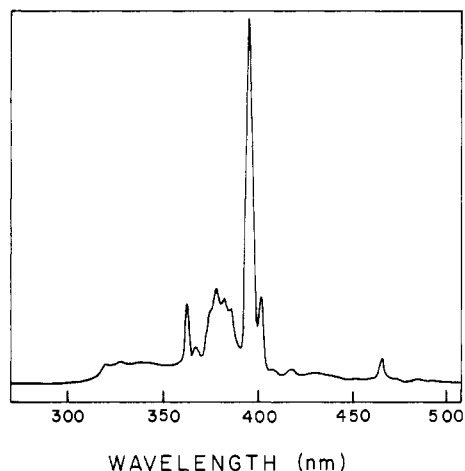


Figure 3. Excitation spectrum of EuDOTMA, obtained at an emission wavelength of 589 nm. The intense feature at 394 nm corresponds to the Eu(III) ${}^7F_0 \rightarrow {}^3L_6$ absorption.

Circular dichroism spectra were recorded on either a modified Cary 60 ORD/CD spectrometer or a Jobin-Yvon Auto-dichrograph Mark V spectrometer. Absorption spectra were measured on a Varian 219 UV/vis spectrophotometer, and specific rotations at 5890 Å were measured with the JASCO optical rotatory dispersion spectrometer (Model ORD/UV-5).

Proton NMR spectra were recorded on a Varian A-360 spectrometer, and ${}^{13}\text{C}$ spectra were obtained on a Bruker HFX-90 spectrometer. NMR shifts to low fields were taken as positive shifts.

Results and Discussion

A. Excitation Spectra of EuDOTMA and TbDOTMA. As many of the investigations carried out on the lanthanide DOTMA complexes involve applications of luminescence spectroscopy, it is important first to detail the excitation spectra of the Tb(III) and Eu(III) complexes. The spectra obtained for aqueous solutions of the complexes are shown in Figures 2 and 3. The TbDOTMA excitation spectrum consists of a series of Tb(III) f-d transitions, and there do not appear to be any excitation features assignable to energy transfer from the DOTMA ligand. The weak excitation at 490 nm corresponds to an f-f absorption of Tb(III) and is due to the ${}^7F_6 \rightarrow {}^5D_4$ transition.

In the EuDOTMA spectrum, all the observed features are due to f-f absorptions associated with the Eu(III) ion, and

Table I. Photophysical Parameters Obtained for the TbDOTMA and EuDOTMA Compounds

TbDOTMA emission lifetime, μs	1450 (H_2O), 2025 (D_2O)
EuDOTMA emission lifetime, μs	405 (H_2O), 690 (D_2O)
Stern-Volmer quenching constants, L/mol:	112, 105
K_{sv}^ϕ, K_{sv}^τ	
bimolecular quenching constant	7.25×10^4
k_q, s^{-1}	

these are easily identified from a comparison to the known free-ion values. The weak feature at 465 nm arises from an absorption from the 7F_0 ground state to the 3D_2 excited state. The 401-nm peak is due to absorption to the 5D_3 state, the 394-nm peak (strongest in the spectrum) is due to absorption to the 5L_6 state, the broad feature centered around 380 nm is due to transitions to the 5G_2 and 5G_6 excited states, and the 362-nm peak is due to an absorption to the 5D_4 excited state. The broad, weak excitation system at higher energy yet is due to absorption bands into many overlapping f states of the Eu(III) ion. Once again, there is no evidence that energy may be absorbed by the DOTMA ligand and subsequently transferred to the Eu(III) ion.

B. Intermolecular Energy Transfer from TbDOTMA to EuDOTMA. Any correlation of chiroptical spectra with a plausible compound structure first requires an understanding of the solution-phase properties of that metal complex. With lanthanide compounds, the highly labile nature of the complexes coupled with the nondirectional bonding associated with the metals often leads to the existence of complicated solution structures. For instance, with carboxylate complexes (especially under basic pH conditions) one often encounters polynuclear species.¹⁴ However, we have developed a spectroscopic method based on intermolecular energy transfer that is capable of determining whether a given lanthanide complex remains monomeric in solution or whether it self-associates into some sort of polymeric compound.^{15,16}

It was in fact observed that addition of EuDOTMA to a solution of TbDOTMA resulted in a decrease both in the Tb(III) emission intensity and in the Tb(III) emission lifetime. If I_0 and τ_0 represent the emission intensity and lifetime of TbDOTMA in the absence of any quencher and I and τ represent the same quantities in the presence of the EuDOTMA quencher, then the quenching results may be quantified by the Stern-Volmer equations

$$(I_0 - I)/I = K_{sv}^\phi[\text{EuDOTMA}] \quad (1)$$

$$(\tau_0 - \tau)/\tau = K_{sv}^\tau[\text{EuDOTMA}] \quad (2)$$

If the energy-transfer process is purely collisional in nature (referred to as dynamic quenching), then it will follow that

$$K_{sv}^\phi = K_{sv}^\tau \quad (3)$$

On the other hand, should the donor and acceptor complexes associate to some extent, it will follow that

$$K_{sv}^\phi > K_{sv}^\tau \quad (4)$$

The rate constant for the dynamic bimolecular quenching is calculable from the lifetime-quenching results:

$$k_q = K_{sv}^\tau/\tau_0 \quad (5)$$

The emission intensity and lifetime results were analyzed by the Stern-Volmer equations, and each plot was found to be absolutely linear to at least a EuDOTMA concentration

(13) Horrocks, W. D.; Sudnick, D. R. *J. Am. Chem. Soc.* **1979**, *101*, 334.

(14) Prados, R.; Stadtherr, L. G.; Donato, H.; Martin, R. B. *J. Inorg. Nucl. Chem.* **1974**, *36*, 689.

(15) Brittain, H. G. *Inorg. Chem.* **1978**, *17*, 2762; **1979**, *18*, 1740.

(16) Brittain, H. G. *J. Inorg. Nucl. Chem.* **1979**, *41*, 561, 567, 721, 1775.

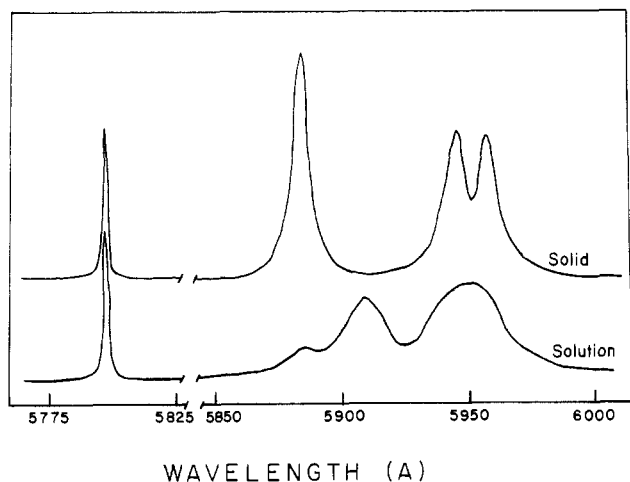


Figure 4. High-resolution emission spectra obtained within the $^5D_0 \rightarrow ^7F_0$ and $^5D_0 \rightarrow ^7F_1$ Eu(III) transitions for microcrystalline EuDOTMA (upper trace) and for EuDOTMA present in a 0.1 M aqueous solution (lower trace). Both spectra were obtained at room temperature.

equal to 10% of that of TbDOTMA. The computed photophysical parameters have all been collected in Table I. One may note that there is a small difference in the Stern-Volmer constants as calculated from the intensity and lifetime data but that this difference is close to only 6%. This value is very close to the experimental error associated with the method, and thus it is most likely that all of the DOTMA complexes are present in a monomeric form.

C. Determination of the Number of Coordinated Water Molecules. In Table I, the emission lifetimes of TbDOTMA and EuDOTMA dissolved in H_2O and D_2O have been provided. From these values, it is possible to calculate the observed emissive rate constants by approximating this value as the reciprocal of the observed lifetime. In H_2O , we thus find that $k_{Eu} = 2.47 \text{ ms}^{-1}$ and $k_{Tb} = 0.69 \text{ ms}^{-1}$, and in D_2O it was found that $k_{Eu} = 1.45 \text{ ms}^{-1}$ and $k_{Tb} = 0.47 \text{ ms}^{-1}$. Horrocks and Sudnick¹³ have shown that the difference between the excited-state reciprocal lifetimes is proportional to the number of coordinated water molecules in the lanthanide complexes. One may then calculate these differences, and we have found that $\Delta k_{Eu} = 1.02 \text{ ms}^{-1}$ and $\Delta k_{Tb} = 0.22 \text{ ms}^{-1}$. According to the published correlation,¹³ one may then conclude that a single water molecule is coordinated by the lanthanide ions in each of the TbDOTMA and EuDOTMA complexes. Such a conclusion is in excellent agreement with the results of the crystal structure on the EuDOTA complex⁸ and with the NMR results.⁴ A similar result was reached by Horrocks et al. in their study of the EuDOTA complex.⁶

D. High-Resolution Luminescence Spectra of EuDOTMA. The effective site symmetry of the Eu(III) ion in EuDOTMA may be deduced from an analysis of the high-resolution luminescence spectrum of this compound. It is clear that the emitting 5D_0 level cannot be split by any crystal field, and thus the number of transitions to the various 7F_j ground levels must reflect the degeneracy of the ground terms. For instance, the $^5D_0 \rightarrow ^7F_0$ transition cannot be split by any crystal field, and thus the number of peaks in this spectral region is indicative of the number of nonoctahedral emitting Eu(III) species present in the sample. We may take this number as being equal to the actual number of species present, since it is known beforehand that the Eu(III) compound symmetry can only be axial at the highest. For each of the other $^5D_0 \rightarrow ^7F_j$ transitions, one may simply compare the number of observed peaks for each band system with published tables¹⁷ to obtain the site

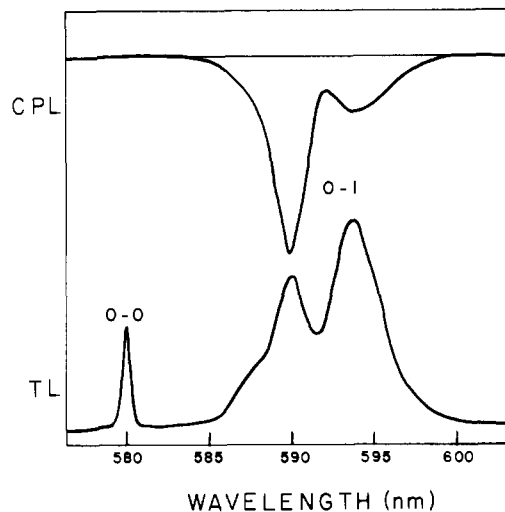


Figure 5. Total luminescence (lower trace) and circularly polarized luminescence (upper trace) spectra obtained within the $^5D_0 \rightarrow ^7F_0$, 7F_1 emission bands of EuDOTMA. The spectra are shown in arbitrary units.

symmetry of the emitting Eu(III) species.

The octadentate DOTMA ligand coordinates as a square antiprism (symmetry D_{4d}), and the capping by the coordinated water molecule reduces the holo-hedrized symmetry to C_{4v} at the highest. The actual site symmetry of the Eu(III) ion would probably be much lower than C_{4v} .

The spectra obtained for EuDOTMA in aqueous solution and as a microcrystalline solid are shown in Figure 4. For purposes of discussion, only the spectra corresponding to the $^5D_0 \rightarrow ^7F_0$, 7F_1 transitions are required. In the crystalline solid, a single sharp $^5D_0 \rightarrow ^7F_0$ band is noted, and the $^5D_0 \rightarrow ^7F_1$ band system clearly consists of three peaks. The data therefore indicate that the metal ion site symmetry cannot be C_{4v} and must be no higher than C_{2v} . The spectra obtained within the $^5D_0 \rightarrow ^7F_3$, 7F_4 band systems are consistent with this conclusion. The overall symmetry of the EuDOTMA complex in the solid must be C_2 or lower (since four asymmetric carbon atoms are present on the DOTMA ligand), but as far as the Eu(III) f-electron states are concerned, one could speak of an effective C_2 site symmetry.

However, when one dissolves the EuDOTMA compound in water, new bands appear within the $^5D_0 \rightarrow ^7F_1$ band system (at 5909 Å, for example) and the $^5D_0 \rightarrow ^7F_0$ band becomes broader. This result indicates that a new species has formed upon dissolution of the complex. Further evidence regarding a real difference between solid-state and solution-phase structures is evident in the enormous decrease in intensity noted for the 5885-Å band and in the collapsing of the 5946/5958 Å doublet into a single broad band centered around 5950 Å. It is quite clear, therefore, that in the aqueous phase, the EuDOTMA complex is actually present as a mixture of two chemically distinct species. The same conclusion was reached by Horrocks et al.⁶ in their work involving EuDOTA complexes, and thus in the present work we have demonstrated the generality of this phenomenon. A quantitative analysis of the structure of the two species present in solutions of YbDOTA and of YbDOTMA will be discussed in the section devoted to the NMR spectra.

The discussion of the observed chirality in the DOTMA complexes must be tempered by the fact that one must deal with the presence of at least two species in the aqueous solutions and that these two species might possess vastly differing chiralities. However, the results of the energy-transfer experiments indicated that both species were monomeric in nature, and the water-counting experiments demonstrated that only a single water molecule was bound by the solution species.

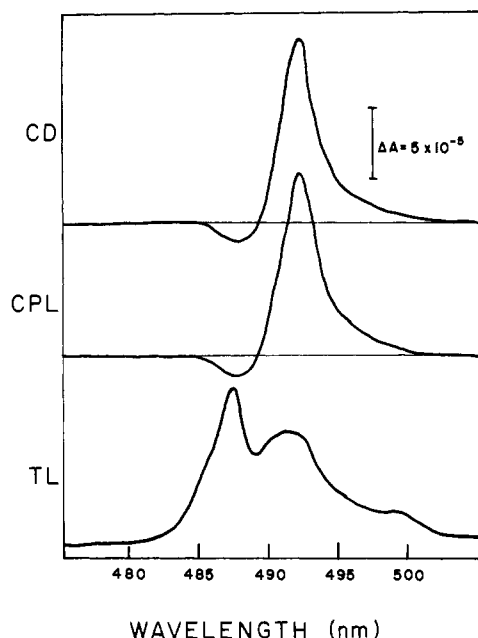


Figure 6. Circular dichroism spectrum (uppermost trace) obtained within the ${}^7F_6 \rightarrow {}^5D_4$ absorption of TbDOTMA, at a concentration of 0.1 M. Total luminescence (lower trace) and circularly polarized luminescence (middle trace) spectra are shown in arbitrary units for the ${}^5D_4 \rightarrow {}^7F_6$ luminescent transition.

E. Circularly Polarized Luminescence Spectra of EuDOTMA. Total luminescence and circularly polarized luminescence spectra obtained within the $D_0 \rightarrow F_0, F_1$ band systems of EuDOTMA in aqueous solution are shown in Figure 5. One may immediately note that the CPL spectrum is dominated by a large peak located at 5909 Å and that the CPL associated with the 5950-Å transition is considerably weaker. Since we have established that the 5909-Å emission band is due to the new species formed upon dissolution of crystalline EuDOTMA, it is not unreasonable to conclude that this peak is indeed due to a complex not possessing axial symmetry. The peak persisting at 5950 Å (and present in the crystalline solid) is thus assigned as originating from the axially symmetric compound identified in the crystal structure.

TL and CPL spectra were recorded within the ${}^5D_0 \rightarrow {}^7F_2, {}^7F_3, {}^7F_4$ band systems, and these have been collected in the supplemental section of the journal. No clear distinction between the two species now identified in solution was present

in these band systems, but this result is clearly a result of the higher degeneracy present in the transitions to levels characterized by high J quantum numbers.

F. Circular Dichroism and Circularly Polarized Luminescence Spectra of TbDOTMA. The TL and CPL spectra associated with TbDOTMA solutions were found to be exceedingly intense, and excellent signal-to-noise ratios were attainable for all ${}^5D_4 \rightarrow {}^7F_J$ ($J = 1-6$). However, since we have now demonstrated that the lanthanide DOTMA complexes exist as two forms in solution, correlation of observed spectra with plausible complex structures is clearly impossible. Consequently, the observed CD and CPL spectra cannot be treated in a quantitative manner. The TL and CPL spectra associated with most of the Tb(III) transitions may be found in the supplemental section of this journal.

One highly significant point may be made, however. As mentioned earlier, the ${}^7F_6 \rightarrow {}^5D_4$ transition may be observed in the absorption or excitation spectrum of TbDOTMA. Upon UV excitation of TbDOTMA, emission from the 5D_4 excited state to the 7F_6 ground state may also be observed. The CD within the ${}^7F_6 \rightarrow {}^5D_4$ band is a reflection of the chirality associated with the 7F_6 ground state, and the CPL associated with the ${}^5D_4 \rightarrow {}^7F_6$ band system is a measure of the chirality of the 5D_4 excited state. One merely has to compare the CD and CPL spectra associated with these transitions to determine the extent of any geometry change that occurs when the complex is placed in an excited f state.

This comparison has been made in Figure 6. It is easily seen that the CD associated with the ${}^7F_6 \rightarrow {}^5D_4$ absorption is absolutely identical in line shape with the CPL associated with the ${}^5D_4 \rightarrow {}^7F_6$ emission. This exact correlation is quantitative as well; the anisotropy factors (defined as the ratio of CPL:TL or CD:ABS) are the same to within experimental error. One may therefore conclude that *no* geometry change accompanies the promotion of the Tb(III) ion into an excited f state. This conclusion is in accord with the accepted view of f orbitals as being essentially nonbonding in nature.

G. NMR Studies of YbDOTA and YbDOTMA. A detailed analysis of the NMR spectra of the lanthanide DOTMA complexes provides further insight into the structure and solution behavior of these compounds. For the sake of comparison, several new considerations on the spectra of the DOTA complexes will be included. Indeed, the DOTA ligand forms nonlabile complexes with the lanthanides^{4,8} that are expected to be very similar to those formed by DOTMA. The studies reported by Horrocks et al.⁶ enabled these workers to conclude from their luminescence studies that EuDOTA adopts

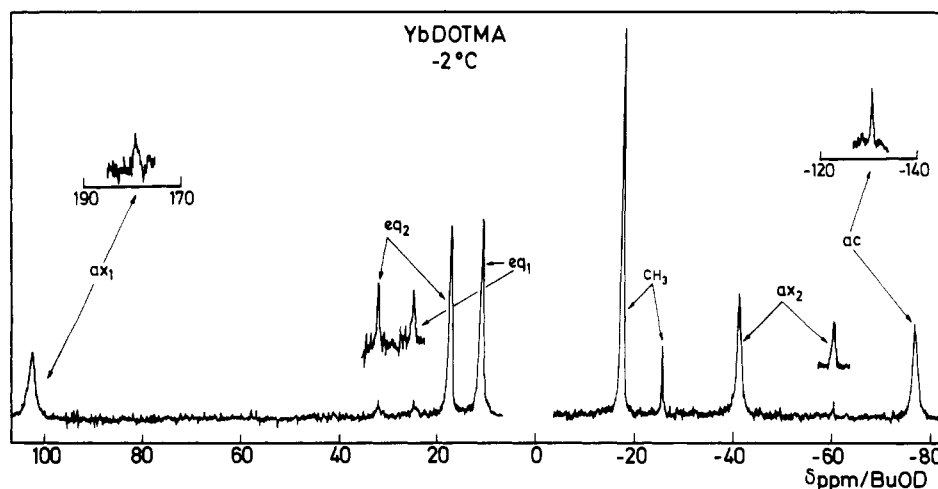


Figure 7. Proton NMR spectrum of YbDOTMA at -2°C . Some of the peaks of the minor YbDOTMA component are reproduced with an enhanced intensity. Assignments: ax1 and ax2 = ring protons in the axial positions; eq1 and eq2 = ring protons in the equatorial positions; ac = acetate proton; CH = α -methyl substituent of the acetate groups.

two different structures in solution. This conclusion is supported by the presence of small NMR resonances, which are observed along with the high-intensity peaks attributed to the axially symmetric species.^{4,6} As mentioned earlier, the luminescence and CPL results reported in the present work also point to the appearance of a new species when EuDOTMA is dissolved in water.

A representative proton NMR spectrum of an aqueous YbDOTMA solution is presented in Figure 7. Each intense resonance is accompanied by a smaller one, and this observation indicates that YbDOTMA is present in solution as two forms that are in slow exchange. The assignments of the NMR resonance lines for both the major and minor components were made from their relative peak areas and by comparison with the spectral data previously reported for YbDOTA.⁴ For YbDOTA, it was shown that all the ethylenediamine groups of the DOTA macrocyclic ring adopt the same fully staggered conformation and are rigid on the NMR time scale. This phenomenon results in the inequivalence of the four types of protons present on the ethylenediamine groups. In the present work, it has been found that YbDOTMA is also conformationally rigid on the NMR time scale. Its proton NMR spectrum consists of two series of four ethylenic peaks (labeled ac and eq in Figure 7), one acetate peak (ac), and one methyl peak (CH₃). The YbDOTA and YbDOTMA complexes exhibit the same spectral properties with one notable exception: the small peaks exhibited by YbDOTA are less shifted than the large peaks, and the reverse situation is noted for YbDOTMA. It should be mentioned that the NMR peaks of the minor form of YbDOTMA span an unusually large chemical shift range of nearly 350 ppm.

Another difference between the two macrocyclic ligands was revealed by a detailed analysis of the values of the induced paramagnetic shifts. In cases of axial symmetry, the dipolar shifts ($\Delta\nu_i$) can be expressed as the product of a magnetic susceptibility factor (D_1) and a mean geometric coefficient:¹⁸

$$\Delta\nu_i = D_1 \left\langle \frac{3 \cos^2 \theta_i - 1}{r_i} \right\rangle \quad (6)$$

where θ_i and r_i are the polar coordinates of a ligand nucleus i with respect to the principal axis of symmetry of the complex. The reliability of a geometrical model can be assessed by comparing the experimental shifts ($\Delta\nu_i^{\text{exptl}}$) with calculated shifts ($\Delta\nu_i^{\text{calcd}}$), the latter simply being the geometric coefficients scaled against the experimental shifts. Willcott et al.¹⁹ suggested that this comparison is best performed by computing the agreement factor:

$$R = \left[\frac{\sum w_i (\Delta\nu_i^{\text{calcd}} - \Delta\nu_i^{\text{exptl}})^2}{\sum w_i (\Delta\nu_i^{\text{exptl}})^2} \right] \quad (7)$$

where w_i is the weighting factor of nucleus i . In the present analysis, equal weighting factors have been used for all peaks. This method of analysis requires that the contact contributions to the experimental shifts be negligible, which then dictates the choice of ytterbium as the paramagnetic probe.^{4,18}

It was reported previously¹⁸ that there was an excellent agreement between all the experimental shifts of the major YbDOTA component and the shifts calculated from the solid-state structure of EuDOTA. As shown in Table II, an agreement factor of $R = 3.6\%$ was computed for $T = -2^\circ\text{C}$. This agreement is significantly lower for the minor YbDOTMA component ($R = 11.1\%$). Examination of Dreiding

Table II. Experimental and Calculated Induced NMR Shifts (ppm) of the Minor and Major YbDOTA and YbDOTMA Species

	$(3 \cos^2 \theta - 1)/r^3$ ^a	minor form		major form	
		exptl	calcd	exptl	calcd
YbDOTA ^b					
ax1	2.904×10^{-2}	84.7	89.6	146.0	147.6
ax2	-1.015×10^{-2}	-37.2	-31.3	-53.2	-51.6
eq1	4.444×10^{-3}	8.6	13.7	19.7	22.6
eq2	5.423×10^{-3}	13.2	16.7	24.7	27.6
ac1	-8.007×10^{-3}	-32.3	-24.7	-45.6	-40.7
ac2	-1.873×10^{-2}	-61.2	-57.8	-96.1	-95.2
$R, \%$		11.1		3.6	
D_1 ^d		3086 ± 395		5082 ± 209	
YbDOTMA ^b					
ax1	2.904×10^{-2}	177.3	176.7	101.6	104.1
ax2	-1.015×10^{-2}	-62.3	-61.8	-43.0	-36.4
eq1	4.444×10^{-3}	23.8	27.0	9.8	15.9
eq2	5.423×10^{-3}	31.0	33.0	16.3	19.4
CH ₃	-4.017×10^{-3}	-25.6	-24.4	-17.4	-14.4
ac	-2.191×10^{-2}	-133.2	-133.3	-80.2	-78.5
$R, \%$		1.7		7.55	
D_1 ^d		6085 ± 121		3585 ± 311	

^a Mean values calculated from the solid-state structure of EuDOTMA¹ except in the case of the peaks labeled CH₃ and ac. For the latter, the geometric factors were obtained by a best-fit treatment. ^b NMR shifts to low fields are taken as positive shifts. Induced shifts are relative to diamagnetic LuDOTA or LuDOTMA; $T = -2^\circ\text{C}$. ^c Nonweighted agreement factor; see eq 6. ^d See eq 5; D_1 in units of ppm Å, errors with a 95% confidence level.

models of YbDOTMA revealed that steric crowding precludes the α -methylacetate groups of the ligand from occupying the same position as the acetate groups of YbDOTA. As a result, the agreement factor was computed for a model that considered only the ring protons. An R value of 8.7% was obtained for the major YbDOTMA component, and a value of 2.0% was calculated for the minor component. It is important to note here that neglecting the acetate peaks of YbDOTA in the computation of the agreement factors only slightly alters the values ($R = 2.7\%$ for the major species and $R = 9.6\%$ for the minor species). All of these R values compare well with the values of the agreement factors reported so far for the limited number of situations where both the crystallographic structure and the NMR spectrum of a rigid lanthanide complex are available. For instance, an analysis of the ¹H and ¹³C spectra of the axially symmetric tris(pyridine-2,6-dicarboxylate) complexes yielded an agreement factor of $R = 3.5\%$.²⁰ Higher values ($R = 8.4$ – 10.1%) were obtained in a multinuclear NMR study of tris[hydridotris(pyrazol-1-yl)borato]ytterbium(III), a complex approximating C_{2v} symmetry.²¹ In comparison with these data, the agreement between the solid-state structure of EuDOTA and the spectra of any of the YbDOTA or YbDOTMA components is fairly good. The fact remains, however, that the R factors of the major YbDOTA and minor YbDOTMA components are 2–4 times smaller than the factors calculated for the other species. These two components are also those that exhibit the largest degree of chemical shift.

Because of their low R values, the major YbDOTA and minor YbDOTMA components are considered to be exactly axially symmetric in solution, and the structure of the latter species can be completely described after a quantitative analysis of the NMR data. Each acetate group present in the distorted square-antiprismatic structure of EuDOTA⁸ was replaced by an α -methylacetate group with the help of a

(18) (a) Inagaki, F.; Miyazawa, T. *Prog. Nucl. Magn. Reson. Spectrosc.* **1981**, *14*, 67. (b) Reuben, J.; Elgavish, G. A. *Handb. Phys. Chem. Rare Earths* **1979**, *4*, 483.
(19) Willcott, M. R.; Lenkinski, R. E.; Davis, R. E. *J. Am. Chem. Soc.* **1972**, *94*, 1742.

(20) Reilley, C. N.; Good, B. W.; Desreux, J. F. *Anal. Chem.* **1975**, *47*, 2110.
(21) Stainer, M. V. R.; Takats, J. J. *Am. Chem. Soc.* **1983**, *105*, 410.
(22) Desreux, J. F.; Loncin, M. F., to be submitted for publication.
(23) Baisden, P. A.; Choppin, G. R.; Garret, B. B. *Inorg. Chem.* **1977**, *16*, 1367 and references cited therein.

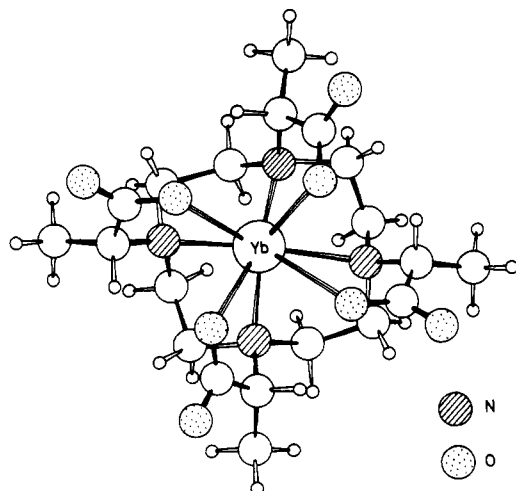


Figure 8. Calculated structure of the minor YbDOTMA species. The carboxylate groups are pointing upward, and the conformation of the macrocyclic ring is identical with the conformation shown in Figure 1 of ref 4.

computer program described previously.²⁴ The position of each α -methylacetate group was then varied systematically until the best agreement with the experimentally observed shifts was obtained. The data collected in Table II were obtained for a mean Yb–N–CH–CH₃ torsion angle of 178°, with the α -methyl groups thus being fully staggered relative to the macrocyclic ring. Consideration of these results indicates that such an orientation of the α -methyl substituents can only be achieved if the conformation of the acetate groups as existing in EuDOTA is inverted. This inversion is equivalent to a rotation of the square face of the antiprismatic structure by 70°. A perspective view of the structure of the axially symmetric isomer of YbDOTMA is shown in Figure 8. For comparison purposes, the complex has been presented in an orientation close to the one selected for EuDOTA in Figure 1 of ref 4. The shifts calculated for the complete structure are compared with the experimental shifts of Table II, with a low value of the agreement factor ($R = 1.7\%$) being obtained.

As indicated in Table II, an agreement factor of $R = 7.5\%$ was calculated for the major YbDOTMA component with the assumption that this species also adopts the axially symmetric structure presented in Figure 8. Once again, this R value is reasonably low but is significantly higher than in the case of the component that exhibits larger shifts. The following question now arises: What could be the structure of the minor YbDOTA and the major YbDOTMA components, the two species with the highest R values and the lowest susceptibility factors, D_1 ? The tetraaza cycle of EuDOTA is exceedingly rigid on the NMR time scale, and it exhibits a strong conformational preference as do all 12-membered macrocycles.⁴ Therefore, an alteration of the conformation of the macrocyclic ring seems unlikely. The presence of an isomer with a dodecahedral structure is ruled out since this would imply a modification of the conformation of the tetraaza macrocycle and because it would lead to the appearance of four NMR acetate peaks instead of two.²² Because of the large differences between the D_1 factors of the various species, the presence of partially uncoordinated carboxylate groups seems more likely. Several studies of linear polyamino polyacetate complexes have indicated that the lifetime of lanthanide–oxygen bonds can

be short on the NMR time scale, while the metal–nitrogen bonds remain nonlabile.²³ The steric crowding of the DOTA and DOTMA complexes could favor the partial release of some carboxylate groups, and such a process would be more likely for the more crowded DOTMA ligand. Average structures differing only slightly from axial symmetry would exist only for the situation where there was fast exchange between the free and bound carboxylate groups.

The values of the susceptibility factors, D_1 , of these average structures are difficult to estimate. Although a subject of some controversy,²⁴ the simplified treatment proposed by Bleaney²⁵ is now widely regarded^{18,24} as sufficiently accurate as to account for the paramagnetic shifts induced by the lanthanides. According to Bleaney, the shifts induced in axially symmetric complexes depend on the crystal field coefficient $\langle r^2 \rangle A_2^0$. Crystal field coefficients are usually regarded as adjustable parameters, but in a simple point charge model, A_2^0 is a function of $\sum_i (3 \cos^2 \theta_i - 1) / r_i^3$, where r_i and θ_i are the spherical polar coordinates of the charges in the first coordination sphere of the lanthanide ion.²⁶ This very approximate model has been used with some success by Zolin et al.²⁷ to determine the sign of the susceptibility factors of various shift reagents, but it is difficult to determine the scope of its validity. The sign of the D_1 factor (when calculated by taking into account the position of the carboxylate groups of DOTA and DOTMA) is in agreement with the sign deduced from the NMR spectra. The lower values of the D_1 coefficients of the minor YbDOTA and of the major YbDOTMA species are thus tentatively ascribed to the partial dissociation of carboxylate groups.

The EuDOTA and EuDOTMA complexes also exhibit two series of NMR peaks (indicating that these also exist in solution as two forms), but the large contact shifts⁴ preclude any interpretation in terms of agreement factors. However, on the basis of the line of reasoning given earlier, the new $^5D_0 \rightarrow ^7F_1$ peak that appears in the luminescence spectrum at 5909 Å upon dissolution of EuDOTMA is assigned to the nonsymmetrical major component of the solution.

Finally, it should be noted that, in the structure depicted in Figure 8, steric interactions between the α -methyl groups and the equatorial ring protons are minimized but the ligand is very tightly packed and contains little flexibility. It has already been reported⁴ that the inversion of the configuration of the ethylenediamine groups of DOTA complexes is slow around 0 °C. Thus, two ¹³C ethylenediamine peaks are observed at that temperature in the spectrum of LaDOTA, and this situation arises since there are two sets of inequivalent carbon atoms in the rigid macrocyclic ring. At higher temperatures, the two peaks coalesce and a free energy of activation equal to 60.7 kJ/mol was obtained by computer simulation. This energy is the highest ever reported for a conformational process taking place in a lanthanide complex, but the DOTMA compounds are probably even more rigid. Indeed, two ethylenediamine ¹³C peaks were observed in the spectrum of LaDOTMA at all temperatures between 0 and 100 °C. From the separation between the two signals at 100 °C, it was determined that the free energy of activation must be higher than 77.5 kJ/mol.

Conclusions

While lanthanide ions have found extensive use as spectral probes, there is a lack of reliable model compounds suitable for NMR work.¹⁸ Because of their symmetry and high rigidity, the DOTA and DOTMA compounds appear to be well suited

(24) (a) Horrocks, W. DeW., Jr.; Sipe, J. P., III; Sudnick, D. In "Nuclear Magnetic Resonance Shift Reagents"; Sievers, R. E., Ed.; Academic Press: New York, 1973; p 53. (b) Golding, R. M.; Pyykko, P. *Mol. Phys.* **1973**, *26*, 1389. (c) Cheng, H. N.; Gutowsky, H. S. *J. Phys. Chem.* **1978**, *82*, 914.

(25) Bleaney, B. *J. Magn. Reson.* **1972**, *8*, 91.

(26) Hutchings, M. T. *Solid State Phys.* **1964**, *8*, 91.

(27) (a) Zolin, V. F.; Koreneva, L. G. *J. Struct. Chem. (Engl. Transl.)* **1980**, *21*, 51. (b) Bablushkina, T. A.; Zolin, V. F.; Koreneva, L. G. *J. Magn. Reson.* **1983**, *52*, 169.

for an assessment of the respective merits of various spectroscopic techniques. The conclusions drawn during the course of the present investigation amply demonstrate the utility of combining luminescence work with NMR studies for the determination of the structure and solution behavior of lanthanide complexes.

The luminescence studies permit one to deduce results that would not have been easily obtained through NMR methods. For instance, it was shown that the lanthanide DOTMA compounds exhibit no tendency to self-associate and that these compounds contain a single water molecule bound at the inner sphere of the metal ion. Furthermore, the luminescence studies clearly indicate that a single, well-defined EuDOTMA species exists in the crystalline solid but that two nonequivalent emitting species exist in solution. This latter conclusion was also obtained from the NMR studies. The luminescence techniques cannot permit one to determine the structures of the DOTMA or DOTA complexes in solution, but through the use of NMR spectroscopy it was possible to propose a structure for each isomer present in the solutions. One must remember, however,

that the results are only suggestive of the nature of the two species yielding the highest values of the *R* agreement factors. In addition, it was demonstrated that the compounds experience a considerable degree of steric crowding and that all the isomers were rigid on the NMR time scale.

Acknowledgment. This work was supported by the Camille and Henry Dreyfus Foundation, through a Teacher-Scholar award to H.G.B. J.F.D. is Chercheur Qualifie at the University of Liege and gratefully acknowledges research support from the Fonds National de la Recherche Scientifique of Belgium. The authors thank Dr. Cl. Houssier (University of Liege) for recording some of the CD spectra and Dr. R. W. White (Chemical Abstracts Service, Columbus, OH) for help in naming the DOTMA ligand.

Supplementary Material Available: Total luminescence and circularly polarized luminescence spectra obtained within the $^5D_0 \rightarrow ^7F_2, ^7F_3, ^7F_4$ transitions of EuDOTMA and within the $^5D_4 \rightarrow ^7F_3, ^7F_4, ^7F_5$ transitions of TbDOTMA (6 pages). Ordering information is given on any current masthead page.

Contribution from the Laboratory of Inorganic Chemistry, College of General Education, and Department of Chemistry, Faculty of Science, Nagoya University, Nagoya 464, Japan

Structural Study of Copper(II) Sulfate Solution in Highly Concentrated Aqueous Ammonia by X-ray Absorption Spectra

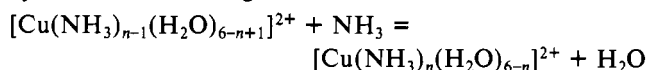
MITSURU SANO,*† TETSUYA MARUO,‡ YUICHI MASUDA,‡ and HIDEO YAMATERA‡

Received February 24, 1984

The structural study of a concentrated ammoniacal solution of copper(II) sulfate has been carried out with X-ray absorption techniques. The EXAFS spectra were obtained for solid $[\text{Cu}(\text{en})_2]\text{Cl}_2 \cdot 2\text{H}_2\text{O}$ and the copper(II) solution in concentrated aqueous ammonia. A comparison of the spectra gives the structural parameters of the copper complex in solution; the Cu-N distance is 2.02 Å, and the coordination number is about 4 as determined by EXAFS. The XANES of the solution suggests a square-pyramidal structure, $[\text{Cu}(\text{NH}_3)_5]^{2+}$. The absorption spectrum has also been considered by using the angular-overlap model. It is concluded that the copper(II) species existing in concentrated aqueous ammonia is a square-pyramidal $[\text{Cu}(\text{NH}_3)_5]^{2+}$ with the bond distance 2.02 Å between copper and equatorial nitrogen atoms.

Introduction

Addition of aqueous ammonia to an aqueous copper(II) solution results in successive replacements of coordinated water by ammonia according to



The successive formation constants have been given for each step of the reactions. K_5 is very small (0.3), and K_6 is practically zero.¹ The electronic spectrum of the aqueous copper(II) solution changes on the addition of aqueous ammonia. The wavenumber and the molar absorption coefficient increase with increasing ammonia concentration until $[\text{Cu}(\text{NH}_3)_4]^{2+}$ is formed. However, further addition of ammonia results in a substantial decrease in the wavenumber of the absorption maximum and a substantial increase in the intensity.

An X-ray diffraction study of solid $\text{K}[\text{Cu}(\text{NH}_3)_5](\text{PF}_6)_3$ has shown a square-pyramidal form for the pentaamminecopper(II) ion with $\text{Cu}-\text{N}_{\text{eq}}=2.010$ and 2.048 and $\text{Cu}-\text{N}_{\text{ax}}=2.193$ Å.² (N_{eq} and N_{ax} denote the equatorial and axial nitrogen atoms.) It is reported from an EXAFS study that $[\text{Cu}(\text{NH}_3)_5](\text{BF}_4)_2$ has five equal Cu-N bond lengths.³ An X-ray diffraction study of the copper(II) species in highly

concentrated ammoniacal solution has been carried out by Yamaguchi et al., who showed a tetragonal structure: $\text{Cu}-\text{N}_{\text{eq}}=1.93$, $\text{Cu}-\text{N}_{\text{ax}}=2.30$, $\text{Cu}-\text{X}_{\text{ax}}=2.30$ Å ($\text{X} = \text{N}, \text{O}$).⁴ This structure is considerably different from that in the crystal.

Extended X-ray absorption fine structure (EXAFS) is well-known to be one of the most powerful tools to study the local environment of a concerned atomic species.⁵ X-ray absorption near-edge structure (XANES) also gives useful information for the molecular geometry.⁶ In this paper, we report a structural study of a copper(II) solution in highly concentrated aqueous ammonia by the X-ray absorption techniques.

Experimental Section

Sample Preparation. An ammoniacal copper solution of high ammonia concentration was prepared by introducing gaseous ammonia into a tetraamminecopper(II) sulfate solution to saturation (the NH_3/Cu mole ratio was about 47). The concentration of the cop-

* Laboratory of Inorganic Chemistry, College of General Education.

† Department of Chemistry.

- (1) Hathaway, B. J.; Tomlinson, A. A. G. *Coord. Chem.* **1970**, *5*, 1-45.
- (2) Alagna, L.; Prosperi, T.; Tomlinson, A. A. G.; Vlais, G. *J. Chem. Soc., Dalton Trans.* **1983**, 645-648.
- (3) Duggan, M.; Ray, N.; Hathaway, B. J.; Tomlinson, A. A. G.; Brint, P.; Pelin, K. *J. Chem. Soc., Dalton Trans.* **1980**, 1342-1348.
- (4) Yamaguchi, T.; Ohtaki, H. *Bull. Chem. Soc. Jpn.* **1979**, *52*, 415-419.
- (5) Sandstrom, D. R.; Lytle, F. W. *Annu. Rev. Phys. Chem.* **1979**, *30*, 215-238.
- (6) Glen, G. L.; Dodd, C. G. *J. Appl. Phys.* **1968**, *39*, 5372-5377.